ELSEVIER

Journal of Power Sources 81–82 (1999) 739–747

JOURNAL OF POWER SOURCES

www.elsevier.com/locate/jpowsour

NMR, DSC and high pressure electrical conductivity studies of liquid and hybrid electrolytes

P.E. Stallworth [a,*], J.J. Fontanella [a], M.C. Wintersgill [a], Christopher D. Scheidler [a], Jeffrey J. Immel [a], S.G. Greenbaum [b], A.S. Gozdz [c]

[a] *Physics Department, US Naval Academy, Annapolis, MD 21402-5026, USA*
[b] *Hunter College of the CUNY, New York, NY 10012, USA*
[c] *Bellcore, 331 Newman Springs Road, Red Bank, NJ 07701, USA*

Abstract

Electrical conductivity, differential scanning calorimetry (DSC) and ^{7}Li nuclear magnetic resonance (NMR) studies have been carried out on liquid electrolytes such as ethylene carbonate:propylene carbonate (EC:PC) and EC:dimethyl carbonate (DMC) containing $LiPF_6$ (and $LiCF_3SO_3$ for NMR) and films plasticized using the same liquid electrolytes. The films are based on poly(vinylidene fluoride) (PVdF) copolymerized with hexafluoropropylene and contain fumed silica. All measurements were carried out at atmospheric pressure from room temperature to about -150°C and the electrical conductivity studies were performed at room temperature at pressures up to 0.3 GPa. The liquids and hybrid electrolytes are similar in that the electrical conductivity of the EC:PC-based substances exhibits Vogel–Tammann–Fulcher (VTF) behaviour while that for the EC:DMC-based substances does not. Part of the deviation from VTF behaviour for the EC:DMC-based materials is attributed to crystallization. Further, the glass transition temperatures as determined from NMR, DSC and electrical conductivity measurements are about the same for the liquids and hybrid electrolytes. However, substantial differences are found. The electrical conductivity of the hybrid electrolytes at room temperature is lower than expected and, more importantly, the relative change of conductivity with pressure is larger than for the liquids. In addition, above the glass transition temperature, the NMR T_1 values are smaller and the NMR linewidths are larger for the hybrid electrolytes than for the liquids while at both low and high temperature the NMR linewidths are larger. Consequently, it is concluded that significant solid matrix–lithium ion interactions take place.

Keywords: Electrical conductivity; Nuclear magnetic resonance; Lithium electrolytes; Activation volume; High pressure

1. Introduction

Rechargeable lithium batteries with hybrid polymeric electrolytes are currently being widely studied [1–13] (this list of references is representative rather than comprehensive). One polymer of interest is poly(vinylidene fluoride) (PVdF). Early work on PVdF includes that of Feullade and Perche [14], Tsuchida et al. [15] and Tsunemi et al. [16]. More recently, Jiang et al. [17] have reported results on this system.

In order to learn more about hybrid electrolytes, differential scanning calorimetry (DSC), electrical conductivity and nuclear magnetic resonance (NMR) studies have been undertaken. The electrical conductivity studies were extended to high pressures. The liquids studied include $LiPF_6$ or $LiCF_3SO_3$ dissolved in various solutions of ethylene carbonate (EC), propylene carbonate (PC) or dimethyl carbonate (DMC). In addition, films were studied which were composed of fumed silica dispersed in PVdF copolymerized with hexafluoropropylene and which were plasticized using the same liquid electrolytes.

Despite the complexity of the system, relatively simple behaviour is observed. For example, many of the new results are interpreted in terms of crystallization and glass formation. These occur to varying degrees depending upon the details of the experiment performed. Further, all behaviour is consistent with the properties of the constituents. For example, PC is a well-known glass-former while EC and DMC crystallize easily and combinations of these behave accordingly. Complications arise because PC can crystallize and EC and DMC can be part of amorphous systems. In addition, inclusion of the polymer and silica in the system produces subtle, yet important effects. In the present paper, electrical conductivity, NMR and DSC mea-

* Corresponding author

0378-7753/99/$ - see front matter
PII: S0378-7753(99)00144-5

Table 1
Summary of the electrical conductivity and its pressure dependence for various electrolytes at room temperature

	σ (mS/cm)	$\partial \ln G/\partial p$ (GPa^{-1})	$\chi_T/3$ (GPa^{-1})	$\partial \ln \sigma/\partial p$ (GPa^{-1})	ΔV (cm^3/mol)
Film:EC:PC:LiPF$_6$	1.2	−7.45	0.3	−7.15	17.7
EC:PC:LiPF$_6$	6.8	−6.44	0.3	−6.14	15.2
Film:EC:DMC:LiPF$_6$	1.3	−7.14	0.3	−6.84	16.9
EC:DMC:LiPF$_6$	11.5	−5.35	0.3	−5.05	12.5

surements are used to elucidate the behaviour of the various systems.

2. Experimental

Two commercial liquids were obtained from EM Industries (Hawthorne, NY). The first was a 1 M solution of $LiPF_6$ dissolved in 1:1 vol (~1:1 mol) EC:PC, and the second sample was also a 1 M concentration of the salt, but dissolved in a 1:1 vol (~0.83:1 mol) EC:DMC. The only liquids prepared in the laboratory were a 1:1 solution of EC:PC, 1:1 solution of EC:DMC and 1 M $LiCF_3SO_3$ in 1:1 EC:PC. These were prepared using 99.7% anhydrous PC, 99% DMC and 98% EC which were obtained from Aldrich Chemical (Milwaukee, WI) and $LiCF_3SO_3$ from Alfa Aesar (Ward Hill, MA). The electrolytes were then used to saturate silica-containing polymer films based on PVdF copolymerized with hexafluoropropylene.

The films were prepared by suspending 3 g of powdered poly(vinylindene-cohexafluoropropylene) (Kynar FLEX (R) 2801 from Elf ATOCHEM NA, King of Prussia, PA), 2 g of silylated fumed silica (TS 530 from Cabot, Billerica, MA) and 5 g of dibutyl phthalate (Aldrich Chemical) in 25 ml of acetone and homogenized for 1 h at room temperature in a laboratory ball mill. The viscous liquid was cast on a glass plate using a doctor blade apparatus, and dried in air. The resulting flexible film was extracted three times in diethyl ether and dried at room temperature. Pieces of the film were then re-swollen for at least 1 h in each of the electrolyte solutions. Mass increases of about 100% were typical.

Prior to measurement, the plasticized films were removed from the liquids and lightly patted with a tissue to remove the surface liquid. All sample preparation and subsequent loading of the samples into various sample holders were carried out in a Vac Atmospheres glove box with less than 0.08 ppm water.

For the electrical measurements, the liquids were placed in Teflon™ coated Tygon™ tubing. One end of the tube was plugged with a gold-coated stainless steel electrode and sealed using a modified SwageLok™ fitting. The liquid to be examined was then placed in the tubing with an eye dropper, and other end of the sample was then plugged with another electrode assembly. A similar arrangement was used for the plasticized films which were measured along the plane of the samples.

The electrical conductivity of the samples at various temperatures was determined by connecting the samples to the cold finger of a Cryogenics Associates CT-14 cryostat. Temperature control was achieved using a Lake Shore Cryotronics DRC-82 temperature controller. This is the same system used previously for a variety of measurements [18–22]. For the high pressure measurements, the samples were connected to the closure plug of the high pressure vessel used previously to measure the effect of

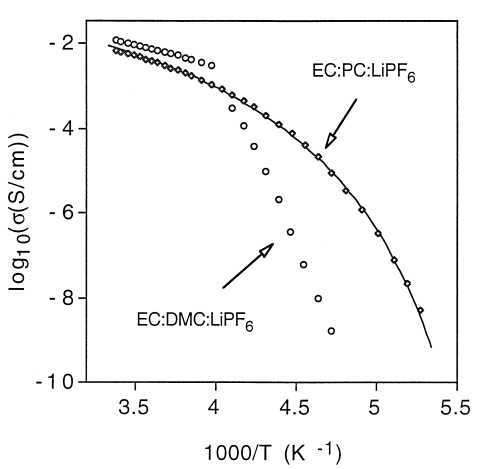

Fig. 1. Electrical conductivity vs. temperature for the liquid electrolytes: EC:PC:LiPF$_6$ (diamonds) and EC:DMC:LiPF$_6$ (circles). Also shown is the best-fit VTF curve (Eq. (3)) for EC:PC:LiPF$_6$.

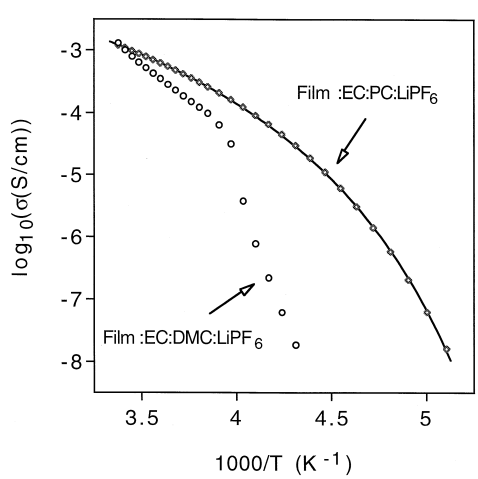

Fig. 2. Electrical conductivity vs. temperature for the hybrid electrolytes: Film:EC:PC:LiPF$_6$ (diamonds) and Film:EC:DMC:LiPF$_6$ (circles). Also shown is the best-fit VTF curve (Eq. (3)) for Film:EC:PC:LiPF$_6$.

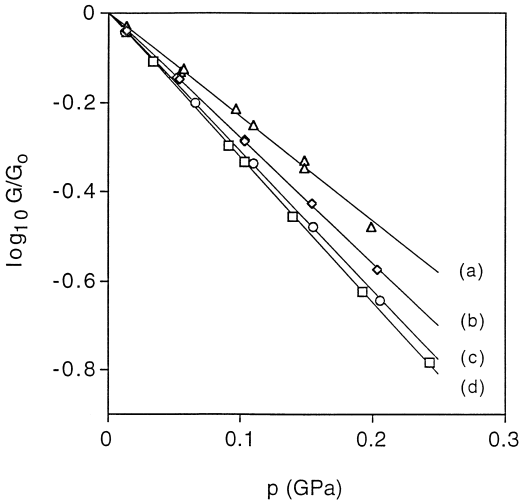

Fig. 3. Relative electrical conductance vs. pressure for (a) EC:DMC:$LiPF_6$; (b) EC:PC:$LiPF_6$; (c) Film:EC:DMC:$LiPF_6$; (d) Film:EC:PC:$LiPF_6$. Also shown are the best-fit straight lines.

high pressure on the electrical conductivity of ion conducting polymers [18,21,23–27]. For both the variable pressure and temperature measurements, the equivalent parallel capacitance and resistance of the sample were then determined using either a CGA-83 capacitance measuring assembly or a Hewlett Packard 4194 A Impedance/Gain-Phase Analyzer which achieve a combined frequency range of 10 Hz to 100 MHz. All data were then transformed to the complex impedance, $Z^* = Z' - jZ''$.

For the NMR measurements, the samples were sealed inside 5 mm diameter Pyrex™ tubes. The ^{7}Li NMR measurements were carried out at ambient pressure using a Chemagnetics CMX-300 spectrometer operating at a frequency of 116 MHz. Dry nitrogen gas was used as a purge. Linewidths were determined from Fourier transformed single pulse responses and spin-lattice relaxation times were obtained from exponential relaxation profiles utilizing a saturation-recovery pulse sequence.

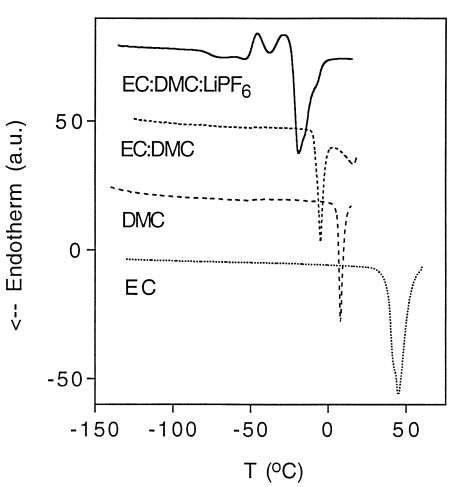

Fig. 4. DSC thermograms for EC, DMC, EC:DMC and EC:DMC:$LiPF_6$.

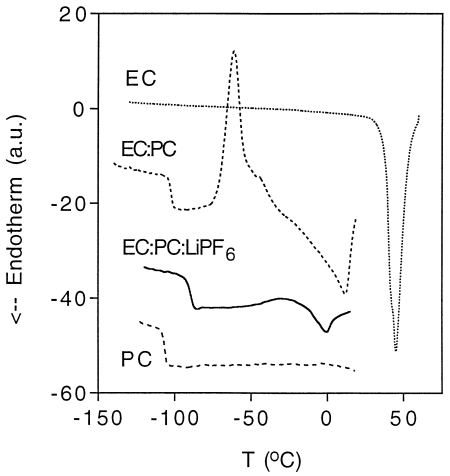

Fig. 5. DSC thermograms for EC, PC, EC:PC and EC:PC:$LiPF_6$.

The DSC measurements were carried out at a scanning rate of 10°C/min using a DuPont Thermal Analyst 2100 with a 910 Cell Base. The DSC measurements for the salt-containing liquids were made using both gold and anodized aluminum pans. No difference was found.

3. Results

For all electrical experiments, a complex impedance diagram consisting of a slightly depressed semicircular arc and slanted line was observed. Those features are usually observed in ion conducting systems such as solvent-free ion conducting polymers with blocking electrodes [18–22]. The bulk resistance, R, was obtained from the intercept of the arc (or position of the minimum value of Z'') or slanted line with the Z' axis. The conductance, $G = 1/R$, was calculated from the intercept. In the case of the room temperature, atmospheric pressure data, the conductance

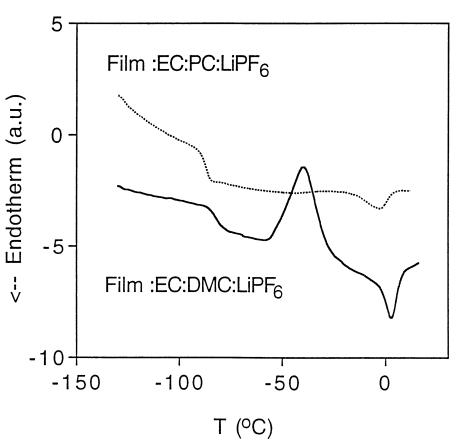

Fig. 6. DSC thermograms for Film:EC:DMC:$LiPF_6$ and Film:EC:PC:$LiPF_6$.

was transformed to the electrical conductivity, σ, via the usual equation:

$$\sigma = GL/A \quad (1)$$

where A is the area of the sample and L is the length. The results are listed in Table 1.

It was found that the EC:DMC:$LiPF_6$ and EC:PC:$LiPF_6$ had conductivities of about 11.5 and 6.8 mS/cm, respectively, at room temperature (approximately 23°C). The value for EC:PC:$LiPF_6$ is in good agreement with the value of 6.56 mS/cm reported for 1 M $LiPF_6$ in 50:50 vol.% EC:PC at 20°C [28]. The conductivity for each associated hybrid electrolyte is lower.

Values of the electrical conductivity at other temperatures and approximately atmospheric pressure were obtained by assuming that the relative change in electrical conductivity is the same as the relative change in electrical conductance, i.e., no correction was made for changes in the dimensions of the sample. The results for the variation of the conductivity with temperature for the liquid and hybrid electrolytes are shown in Figs. 1 and 2, respectively.

The results for the variation of the conductance with pressure at room temperature are shown in Fig. 3. Straight lines were best-fitted to the data and the resultant slopes and intercepts are listed in Table 1. The pressure variation of the electrical conductivity can be calculated from:

$$\left(\frac{\partial \ln \sigma}{\partial p}\right)_T = \left(\frac{\partial \ln G}{\partial p}\right)_T + \frac{\chi_T}{3} \quad (2)$$

where χ_T is the isothermal compressibility. The compressibility for these materials does not seem to be available. However, the compressibility for most liquids is on the order of 0.8–1.2 GPa^{-1} [29]. Consequently, an approximate correction of $\chi_T/3 \cong 0.3\ GPa^{-1}$ was applied to the data and the results are listed in Table 1.

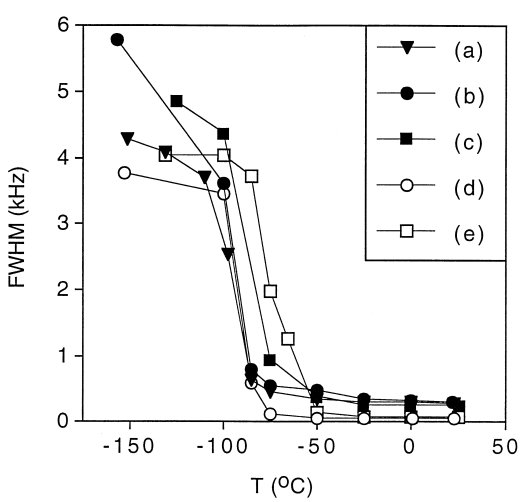

Fig. 7. ^{7}Li linewidth for various materials: (a) Film:EC:PC:$LiCF_3SO_3$; (b) Film:EC:PC:$LiPF_6$; (c) Film:EC:DMC:$LiPF_6$, (d) EC:PC:$LiPF_6$; (e) EC:DMC:$LiPF_6$.

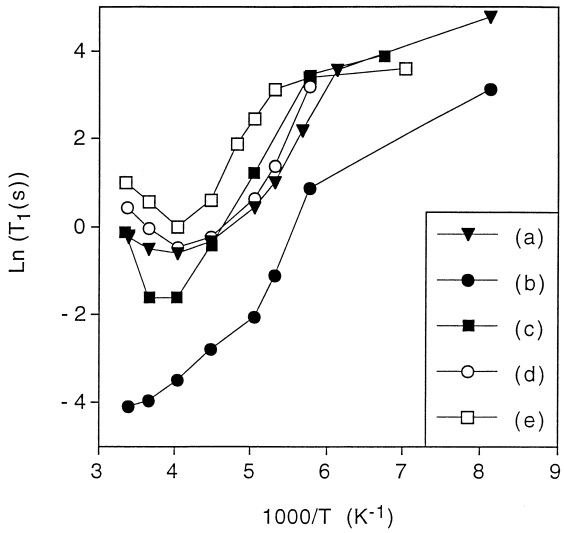

Fig. 8. Natural logarithm of ^{7}Li spin-lattice relaxation time (T_1) vs. 1000/T for various materials: (a) Film:EC:PC:$LiCF_3SO_3$; (b) Film:EC:PC:$LiPF_6$; (c) Film:EC:DMC:$LiPF_6$, (d) EC:PC:$LiPF_6$; (e) EC:DMC:$LiPF_6$.

The results of the DSC runs are shown in Figs. 4–6. The ^{7}Li NMR linewidth results are shown in Fig. 7 and the T_1 data are shown in Fig. 8.

4. Discussion

It is clear from Figs. 1 and 2 that the temperature variation of the electrical conductivity of both EC:PC:$LiPF_6$ and the related hybrid electrolyte is significantly different from that of the EC:DMC:$LiPF_6$-based substances. While the electrical conductivity of the former exhibits a smooth variation with temperature, the latter does not, with the EC:DMC:$LiPF_6$ and associated hybrid electrolyte showing a precipitous drop in the vicinity of −23°C. This behaviour was reproducible under the conditions of the electrical conductivity measurements. However, as discussed below, a discontinuity at −23°C is not observed in the NMR linewidth measurements and, while an event is observed in the vicinity of −23°C in the DSC thermograms other features are also observed.

The interpretation of the difference between the two systems is that, under the conditions of the electrical conductivity studies, as temperature is lowered EC:DMC:$LiPF_6$ and the related hybrid electrolyte undergo crystallization in the vicinity of −23°C while EC:PC:$LiPF_6$-based substances do not, the latter being a glass-forming liquid. This interpretation is consistent with the DSC results shown in Figs. 4–6. It is apparent from Figs. 4 and 6 that all EC- and DMC-based substances exhibit a strong endothermic event typical of melting and for EC:DMC:$LiPF_6$, the melting is observed in the vicinity of −23°C. The position of

the endotherm varies over a range of about 10°C depending upon the conditions of the experiment, cooling rate, etc. Obviously, the DMC-based substances have a tendency to crystallize.

On the other hand, as is apparent from Figs. 5 and 6, all of the PC-based materials show a strong feature typical of a glass transition. For EC:PC:$LiPF_6$ and the related hybrid electrolyte, the glass transition is observed at about −90°C. This is consistent with the data shown in Fig. 7 where it is seen that the ^{7}Li NMR linewidth for the EC:PC:$LiPF_6$-based substances exhibits a rapid rise as the temperature is reduced below about −83°C. This result reflects a similar change in the dynamics of the solvated lithium ions in the liquid and hybrid electrolytes as the temperature is reduced below T_g.

However, at about 0°C, both EC:PC:$LiPF_6$ and the related hybrid electrolyte also exhibit a DSC endotherm typical of melting. This endotherm is preceded by an exotherm which probably represents crystallization. Such an event is not reflected in either the electrical conductivity or NMR linewidth data. That is not surprising, since both the electrical conductivity and NMR experiments are carried out at various temperatures achieved by slowly cooling the sample to the desired temperature then equilibrating so that the data are taken isothermally. The DSC data, on the other hand, are taken while the temperature is increasing at 10°C/min.

Next, a weak glass transition is observed for both EC:DMC:$LiPF_6$ and the associated hybrid electrolyte even though EC:DMC appears to be totally crystalline at low temperature. This is not an unknown phenomenon since in PEO, for example, $NaCF_3SO_3$ and NaI suppress crystallinity in favor of an amorphous structure [27]. It is significant that T_g occurs at a higher temperature both in EC:DMC:$LiPF_6$ and the related hybrid electrolyte than for the EC:PC:$LiPF_6$-based substances since T_g varies from about −67°C to about −76°C. This is confirmed by the ^{7}Li NMR linewidth data shown in Fig. 7. Specifically, while the EC:PC:$LiPF_6$-based substances exhibit a rapid rise in the linewidth when the temperature is reduced below about −90°C, the rise occurs at about 20°C higher for EC:DMC:$LiPF_6$ and about 10°C higher for the associated hybrid electrolyte.

The smooth variation of the electrical conductivity with temperature observed for EC:PC:$LiPF_6$ is not surprising since EC:PC containing other salts has been shown to be a glass-forming liquid and the related smooth variation of such properties as viscosity, electrical conductivity or dielectric relaxation times for one of the constituents, PC, is well-documented [30–37]. A quantitative treatment can be given in terms of the VTF [38–40] equation:

$$\sigma = \sigma_0 \exp\left(\frac{-B}{T - T_0}\right) \tag{3}$$

or the modified VTF equation:

$$\sigma = \frac{A}{\sqrt{T}} \exp\left(\frac{-B'}{T - T_0'}\right) \tag{4}$$

A non-linear least squares procedure was carried out as described elsewhere [41]. The resultant best-fit parameters are listed in Table 2 and the best-fit curves are shown in Figs. 1 and 2.

It is interesting that the values of T_0 or T_0', the 'ideal glass transition temperatures' for EC:PC:$LiPF_6$ and the associated hybrid electrolyte are about −113°C. This is consistent with T_g from both DSC ($T_g = -90$°C) and NMR ($T_g = -83$°C) since T_0 and T_0' are usually 20–50°C below T_g [18,20–23,26,27,35]. Further insight can be obtained by comparing the VTF results to a similar treatment of structural relaxation times and viscosity and by applying both the formalism of Angell [35] and Williams et al. [42] and the theory of Bendler and Shlesinger [43] to the data. That discussion is given elsewhere [36].

The result that the values of the transition temperatures for EC:PC:$LiPF_6$ and the related hybrid electrolyte are approximately the same is another indication that the liquid in the hybrid electrolyte is similar to the pure liquid. In fact, as is apparent from Figs. 5 and 6, the DSC thermograms for EC:PC:$LiPF_6$ and its hybrid electrolyte are essentially identical. However, the DSC data shown in Figs. 4 and 6 show that EC:DMC:$LiPF_6$ and its hybrid electrolyte are different. Even though the glass transition temperatures occur at approximately the same position and there is an exotherm at about the same temperature (−40°C) in both substances, EC:DMC:$LiPF_6$ exhibits a

Table 2
Best-fit VTF parameters for electrical conductivity data

Material	Temperature range (K)	$\log_{10}[\sigma_0$ (S/cm)]	B (K)	T_0 (K)	RMS dev
Film:EC:PC:$LiPF_6$	196–296	−1.03	602	157.3	0.0137
EC:PC:$LiPF_6$	196–296	−0.43	530	161.6	0.0211
EC:PC:$LiPF_6$	190–296	−0.296	579	158.7	0.0354

	Temperature range (K)	$\log_{10}[A$ ($K^{1/2}$ S/cm)]	B' (K)	T_0' (K)	RMS dev
Film:EC:PC:$LiPF_6$	196–296	0.285	634	156.3	0.0123
EC:PC:$LiPF_6$	196–296	0.876	558	160.6	0.0190
EC:PC:$LiPF_6$	190–296	1.00	605	157.9	0.0326

second high temperature exotherm (-30°C) and melting occurs at a different temperature. This behaviour is not surprising since it is expected that crystallization and melting would be particularly sensitive to the environment of the liquid.

However, there are other results which show differences between the bulk liquids and the liquid in the hybrid electrolytes. First, it is clear that the value of the electrical conductivity of the hybrid electrolyte cannot be explained by assuming that the film is an inert insulating material since a detailed analysis of a similar system showed that the hybrid electrolyte has a lower conductivity than that predicted by the Bruggeman formula [3]. One explanation is that the electrical conductivity of the liquid in the plasticized film is lower than that of the bulk liquid. Evidence that this is probably the case is as follows.

For temperatures greater than about -73°C, the NMR linewidths (full-width at half-maximum) are 300–400 Hz for both hybrid electrolytes and about 60–160 Hz for the liquids. In that temperature range, the line broadening due to quadrupolar interactions can be neglected and differences in ^{7}Li linewidths between the hybrid electrolyte and the liquid can be attributed to a combination of magnetic dipolar interactions with protons, ^{7}Li, ^{19}F and ^{31}P nuclei. The smaller linewidths for the liquids reflect the efficient averaging of the dipolar interaction due to rapid lithium ion motion. Therefore, hindered motions of the lithium ions produce relatively larger linewidths as observed with the hybrid electrolytes.

As the temperature is reduced below about -83°C, the distinctions between the liquids and hybrid electrolytes become more apparent. The 'rigid-lattice' linewidths (limiting values) are slightly larger for the hybrid electrolytes than for the liquids (about 4 kHz). The effect of the film is to increase the magnetic dipole contribution on the ^{7}Li line. The general shape of the low-temperature ^{7}Li responses are the same for all samples revealing the $1/2$ to $-1/2$ central transition flanked by the broadened satellite transitions; therefore, the lithium chemical environments are very similar in both the liquids and hybrid electrolytes. Lithium ions probably do not bond directly to the film. Instead, the solid matrix acts indirectly to modify the structure and/or dynamics of the solvation sphere (units of EC:PC, EC:DMC and anion) about the lithium ions. The details of the interaction are not completely known; but, since the magnetic dipolar contribution goes as r^{-3} (r is the dipole–dipole distance), it appears that the film causes the lithium ions to be more 'tightly' bound to their solvation spheres or allows for the anion to reside in closer proximity to the lithium ions. Evidence for anion reassociation with lithium has been given by Cazzanelli et al. [44] in their study of lithium solvation in EC:PC:$LiClO_4$ solutions at large salt concentrations.

Comparison of the low-temperature linewidth behavior shown in Fig. 7 reveals a 1.5 kHz difference between EC:PC:$LiPF_6$ and EC:PC:$LiCF_3SO_3$. This result indicates that significant anion effects exist. Based upon the number of interacting spins, it is reasonable that the PF_6 anion contributes more to the magnetic dipolar interaction than the CF_3SO_3 anion. It is also plausible that residual motions of the solvated lithium species exist when CF_3SO_3 anions are present as opposed to PF_6 anions. These differences would arise from the lithium cation association competition between anions and EC:PC solvent. It must be noted that previous ^{7}Li–^{19}F decoupling studies of EC:PC:$LiAsF_6$ in PMMA show that the dipolar broadening contribution to the ^{7}Li NMR line by surrounding fluorine nuclei is small, suggesting that AsF_6 anions are in rapid motion and/or remotely located such that the lithium ions are solvated by (non-fluorinated) EC and PC molecules [45]. On the other hand, dipolar interactions between ^{7}Li and ^{19}F have been reported for polyethers [46] and PAN [47] complexed with $LiBF_4$, indicating that for these materials the lithium ions reside near to their anion counterparts. Clearly, there are conflicting opinions for related phenomena in electrolyte gels but the situation needs to be clarified and understood in the context of hybrid electrolytes.

Further differences between the liquids and hybrid electrolytes are provided by the temperature dependence of the spin-lattice relaxation times, T_1. In general, the Arrhenius T_1 contours are higher for the liquid samples than for the associated hybrid electrolytes (Fig. 8). This suggests that, for dynamics on the order of 100 MHz, the solvated lithium complexes are more tightly held (i.e., their motions are inhibited). This results in the lower T_1 values in the solid matrix over the liquids. On the other hand, the fact that the T_1 minima for the DMC containing hybrid film and solution electrolytes lie near -23°C may not be greatly correlated with melting as suggested by the DSC results. Instead, this is a general characteristic, shared by all except the EC:PC:$LiPF_6$ hybrid film, and reflects similar dynamics as the transition is made between high and low-temperature relaxation mechanisms.

The solvent effect, observed in the linewidth behavior, is also observed in the T_1 data as well. The T_1 contours for the EC:DMC-based substances are higher than the contours for the EC:PC-based substances. Therefore, the NMR results indicate that DMC has the effect of decoupling the lithium ion from the 'lattice' so that the nuclei do not relax as effectively as when PC is present. Moreover, the T_1 contours for the EC:PC-based liquids and hybrid electrolytes are more broad and U-shaped; whereas, the contours for the EC:DMC-based substances are sharper and V-shaped. This implies that the lithium ion environments in the EC:PC-based substances are more heterogeneous and that the correlation times associated with lithium ion motions are more widely distributed. Such behavior is often observed in vitreous and heterogeneous systems and is supported by the fact that EC:PC:$LiPF_6$ forms glasses easily whereas EC:DMC:$LiPF_6$ does not.

Anion effects are also present in the T_1 results. For temperatures between about $-73°$ and $+25$°C, the relax-

ation times for the EC:PC:$LiPF_6$ hybrid electrolyte are over two orders-of-magnitude smaller than for the EC:PC:$LiCF_3SO_3$ hybrid electrolyte. Therefore, more efficient relaxational processes are present for the former plasticized film due to the different anion. As mentioned in the linewidth results, the solvated lithium ions are possibly more mobile, with increased T_1 values, when the CF_3SO_3 anion is present as opposed to the PF_6 anion.

The glass transition near -83°C is not resolved in the relaxation data for any of the hybrids and solutions. The spin-lattice relaxation times describe motions that are of a much higher frequency than those associated with any polymer segmental motion, for example, and the high frequency couplings between the nuclear spin system and the lattice are greatest when the relaxation times are smallest. The T_1 minimum for the EC:PC:$LiPF_6$ hybrid electrolyte lies above room temperature and therefore was not observed. This implies that ionic motions on the order of 100 MHz are more inhibited at room temperature in this hybrid electrolyte than in any of the liquids or the other plasticized films. However, results from electrical measurements, shown in Fig. 2, are in apparent contradiction since the conductivity of the EC:PC:$LiPF_6$ hybrid film is higher than that of the EC:DMC:$LiPF_6$ hybrid film below room temperature. This indicates that long-range ion mobilities are more restricted for the DMC-based than with the PC-based hybrid film. The interpretation is complicated further by the observation of the opposite behavior of conductivities gathered for the liquids above -23°C. The implication is that long-range motions for the PC-based electrolyte solution are more inhibited (Fig. 1). In light of these facts, it is clear that the NMR T_1 results are governed primarily by short-range ionic motions (such as rotations). Therefore, in comparison with the DMC-based hybrid film, a tight solvation sphere, for lithium ions in the PC-based hybrid film, couples local ionic rotations and vibrations to a greater degree with polymer segmental motions. Additionally, these polymer segmental motions enhance translational motions of the solvated complex. The tendency for the DMC-based materials to crystallize compromises the long-range motion in the film, i.e., the crystallized regions are effectively decoupled from the polymer segmental motions. The onset of crystallization/melting occurs at a higher temperature for the DMC-based film compared to the liquid, and therefore, retardation of long-range ionic motion is initiated at higher temperatures.

In order to discuss the effect of pressure on the electrical conductivity, the 'Arrhenius' activation volume:

$$\Delta V = -kT\left(\frac{\partial \ln \sigma}{\partial p}\right)_T \quad (5)$$

is considered. The values of ΔV, calculated using Eq. (5), are listed in Table 1. As has been discussed elsewhere [18,25,48], the activation volume as defined above is not strictly correct for materials which exhibit non-Arrhenius behaviour. However, it is a useful quantity for comparison with data in the literature.

The effect of pressure on the electrical conductivity of the liquids is consistent with previous results for related liquids [25]. In the previous work, it was found that the activation volume for EC:DMC in a different ratio (2:1) containing various salts ranged from 11.2 to 12.7 cm^3/mol. This overlaps the value of 12.5 cm^3/mol observed in the present work for EC:DMC:$LiPF_6$. The value for EC:PC:$LiPF_6$ is somewhat larger at 15.2 cm^3/mol. An explanation of the larger value of ΔV for EC:PC:$LiPF_6$ is that the molecules fill a larger percentage of the available space than in the case of EC:DMC:$LiPF_6$. Therefore, the activation volume is larger because EC:PC:$LiPF_6$ requires more *change* in volume (which the activation volume represents) in order for the ions to migrate. This is also consistent with the electrical conductivity and NMR results. Specifically, from Table 1, the liquid with the larger electrical conductivity exhibits the smaller activation volume. Again, this is reasonable since the interpretation is that the higher electrical conductivity is a result of the extra volume which is available in EC:DMC:$LiPF_6$. It will be of interest to investigate these liquids containing other salts.

The pressure dependence of the electrical conductivity shows a difference between each liquid and the associated hybrid electrolyte since the activation volume for the hybrid electrolyte is slightly larger than for the liquid. The same trend was observed for gel electrolytes based on poly(acrylonitrile) [25]. This difference cannot be accounted for by a geometrical model and thus again represents a fundamental difference between the liquid and liquid in the associated hybrid electrolyte. The reason is that the pressure variation of either the conductance or conductivity (or activation volume which is calculated using the relative change in conductivity) are quoted as a *relative* change and relative changes are independent of the size and shape of the solid matrix provided that they do not change with the application of high pressure. Consequently, the difference in the pressure dependence between the liquids and associated hybrid electrolytes represents evidence for an interaction between the solid matrix and the mobile ions. This is, of course, consistent with the NMR results discussed above.

Next, it is noted that the correlation between electrical conductivity and activation volume is preserved for all substances. Specifically, the activation volume decreases as the electrical conductivity increases. This probably reflects the similarity in transport mechanism for all substances studied.

Finally, it is of interest to compare the pressure results to those for solvent free ion-conducting polymers. A summary of the previous results for PPO are shown in Fig. 4 of Ref. [13] or Fig. 6 of Ref. [16] where it is seen that the activation volume decreases from about 80 to 20 cm^3/mol over the temperature range of about $70 + T_0$ to $160 + T_0$°C.

Data for PEO [48], amorphous PEO [27], and PDMS:EO [21,22] fall in the same range. Consequently, the results of about 12 to 17 cm^3/mol at about $138 + T_0$°C are somewhat smaller than the values observed for traditional ion-conducting polymers. This probably reflects the difference in transport mechanism between solvent free polymer electrolytes, where large scale segmental motions control electrical transport, and the liquid and hybrid electrolytes studied in the present work.

5. Summary

In summary, several results have been obtained via NMR, DSC and electrical conductivity studies of various liquid and hybrid electrolytes. The liquids and hybrid electrolytes are similar in that the electrical conductivity of the EC:PC-based substances exhibits VTF behaviour while that for the EC:DMC-based substances shows a rapid drop as temperature is lowered below about −23°C. The rapid drop is attributed to crystallization. Further, the glass transition temperatures are about the same for each liquid and associated hybrid electrolyte. However, substantial differences are found. The electrical conductivity of the plasticized films at room temperature are lower than expected and, more importantly, the relative change of conductivity with pressure is larger than for the liquids. In addition, the NMR linewidth is larger for the hybrid electrolytes both above and below T_g. Also, above the glass transition temperature, the NMR T_1 values are smaller for the hybrid electrolytes than for the liquids. These differences, based on experiments with a dynamical range from DC to 100 MHz, suggest that the lithium ion motions are more restricted in the hybrid electrolytes as compared with the bulk liquids. It is concluded that through solvent mediation, polymer–lithium ion interactions take place even with highly concentrated salt solutions (1 M). These interactions are less significant in the event of crystallization, as observed in the case of the DMC-based hybrid film.

Acknowledgements

This work was supported in part by the Office of Naval Research.

References

[1] A.S. Gozdz, J.-M. Tarascon, O.S. Gebizlioglu, C.N. Schmutz, P.C. Warren, F.K. Shokoohi, in: S. Megahed, B.M. Barnett, L. Xie (Eds.), Proceedings of the Symposium on Rechargeable Lithium and Lithium-ion Batteries, Electrochemical Society, Pennington, NJ, 94-28, 1995, p. 400.
[2] J.-M. Tarascon, A.S. Gozdz, C.N. Schmutz, F.K. Shokoohi, P.C. Warren, Solid State Ionics 86–88 (1996) 49.
[3] M. Doyle, A.S. Gozdz, C.N. Schmutz, J.-M. Tarascon, J. Electrochem. Soc. 143 (1996) 1890.
[4] G.B. Appetecchi, F. Croce, B. Scrosati, M. Wakihara, Proceedings of the Symposium on Batteries for Portable Applications and Electric Vehicles, Electrochemical Society, Pennington, NJ, 97-18, 1997, p. 488.
[5] T. Skotheim, Appl. Phys. Lett. 38 (1981) 712.
[6] R.A. Zoppi, C.M.N.P. Fonseca, M.A. De Paoli, S.P. Nunes, Acta Polym. 48 (1997) 193.
[7] A.S. Gozdz, J.-M. Tarascon, C.N. Schmutz, P.C. Warren, O.S. Gebizlioglu, F. Shokoohi, in: H.A. Frank, H. Oman (Eds.), Proc. Ann. Batt. Conf. Appl. Adv., IEEE, New York, NY, Vol. 10, 1995, p. 301.
[8] C. Arbizzani, M. Mastragostino, L. Meneghello, X. Andrieu, T. Vicedo, Mater. Res. Soc. Symp. Proc., Solid State Ionics III 293 (1993) 169.
[9] K. Shigehara, N. Kobayashi, E. Tsuchida, Solid State Ionics 14 (1984) 85.
[10] X.-M. Wang, M. Iyoda, T. Nishina, I. Uchida, J. Power Sources 68 (1997) 487.
[11] C. Borghini, M. Mastragostino, L. Meneghello, P. Manaresi, A. Munari, Solid State Ionics 67 (1994) 263.
[12] M. Oda, S. Higo, Patent: Jpn. Kokai Tokkyo Koho, JP 87278774 A2, JP 62278774, Date: 871203.
[13] A. Yamada, J. Shigehara, Patent: Jpn. Kokai Tokkyo Koho, JP 86254613, JP 61254613, Date: 861112.
[14] G. Feullade, P. Perche, J. Appl. Electrochem. 5 (1975) 63.
[15] E. Tsuchida, H. Ohno, K. Tsunemi, Electrochimica Acta 28 (1983) 591.
[16] K. Tsunemi, H. Ohno, E. Tsuchida, Electrochimica Acta 28 (1983) 833.
[17] Z. Jiang, B. Carroll, K.M. Abraham, Electrochimica Acta 42 (1997) 2667.
[18] J.J. Fontanella, M.C. Wintersgill, J.P. Calame, M.K. Smith, C.G. Andeen, Solid State Ionics 18–19 (1986) 253.
[19] J.J. Fontanella, M.G. McLin, M.C. Wintersgill, J. Polym Sci., Part B: Polym. Phys. 32 (1994) 501.
[20] Y.S. Pak, K.J. Adamic, S.G. Greenbaum, M.C. Wintersgill, J.J. Fontanella, C.S. Coughlin, Solid State Ionics 45 (1991) 277.
[21] M.C. Wintersgill, J.J. Fontanella, M.K. Smith, S.G. Greenbaum, K.J. Adamic, C.G. Andeen, Polymer 28 (1987) 633.
[22] K.J. Adamic, S.G. Greenbaum, M.C. Wintersgill, J.J. Fontanella, J. Appl. Phys. 60 (1986) 1342.
[23] J.J. Fontanella, M.C. Wintersgill, M.K. Smith, J. Semancik, C.G. Andeen, J. Appl. Phys. 60 (1986) 2665.
[24] J.J. Fontanella, C.A. Edmondson, M.C. Wintersgill, Y. Wu, S.G. Greenbaum, Macromolecules 29 (1996) 4944.
[25] C.A. Edmondson, M.C. Wintersgill, J.J. Fontanella, F. Gerace, B. Scrosatti, S.G. Greenbaum, Solid State Ionics 85 (1996) 173.
[26] S.G. Greenbaum, Y.S. Pak, M.C. Wintersgill, J.J. Fontanella, J.W. Schultz, C.G. Andeen, J. Electrochem. Soc. 135 (1988) 235.
[27] M.C. Wintersgill, J.J. Fontanella, Y.S. Pak, S.G. Greenbaum, A. Al-Mudaris, A.V. Chadwick, Polymer 30 (1989) 1123.
[28] J.T. Dudley, D.P. Wilkinson, G. Thomas, R. LeVae, S. Woo, H. Blom, C. Horvath, M.W. Juzkow, B. Denis, P. Juric, P. Aghakian, J.R. Dahn, J. Power Sources 35 (1991) 59.
[29] J. Brandrup, E.H. Immergut (Ed.), Polymer Handbook, Wiley, New York, 1975.
[30] J. Barthel, H.J. Gores, P. Carlier, F. Feuerlein, M. Utz, Ber. Bunsenges. Phys. Chem. 87 (1983) 436.
[31] A. Bondeau, J. Huck, J. Phys. 46 (1985) 1717.
[32] C.A. Angell, J. Phys. Chem. Solids 49 (1988) 863.
[33] J. Huck, A. Bondeau, G. Noyel, L. Jorat, IEEE Trans. Electrical Insulation 23 (1988) 615.
[34] F. Stickel, E.W. Fischer, R. Richert, J. Chem. Phys. 105 (1996) 2043.
[35] C.A. Angell, Polymer 26 (1997) 6261.

[36] J.J. Fontanella, M.C. Wintersgill, J.J. Immel, J. Chem. Phys. 110 (1999) 5392.
[37] P.E. Stallworth, J. Li, S.G. Greenbaum, F. Croce, S. Slane, M. Salomon, Solid State Ionics 73 (1994) 119.
[38] H. Vogel, Phys. Z. 22 (1921) 645.
[39] V.G. Tammann, W. Hesse, Z. Anorg. Allg. Chem. 156 (1926) 245.
[40] G.S. Fulcher, J. Am. Ceram. Soc. 8 (1925) 339.
[41] J.J. Fontanella, M.C. Wintersgill, C.S. Coughlin, P. Mazaud, S.G. Greenbaum, J. Polym. Sci., Polym. Phys. 29 (1991) 747.
[42] M.L. Williams, R.F. Landel, J.D. Ferry, J. Am. Chem. Soc. 77 (1955) 3701.
[43] J.T. Bendler, M.F. Shlesinger, J. Stat. Phys. 53 (1988) 531.
[44] E. Cazzanelli, F. Croce, G.B. Appetecchi, F. Benevelli, P. Mustarelli, J. Chem. Phys. 107 (1997) 5740.
[45] P.E. Stallworth, S.G. Greenbaum, F. Croce, S. Slane, M. Salomon, Electrochimica Acta 40 (1995) 2137.
[46] S.G. Greenbaum, S. Panero, B. Scrosati, Electrochimica Acta 37 (1992) 1533.
[47] F. Croce, S.D. Brown, S.G. Greenbaum, S.M. Slane, M. Salomon, Chem. Mater. 5 (1993) 1268.
[48] J.J. Fontanella, M.C. Wintersgill, J.P. Calame, F.P. Pursel, D.R. Figueroa, C.G. Andeen, Solid State Ionics 9–10 (1983) 1139.